energy. It indicates that the self-assembly of a polymer on an atomically flat substrate could be a new route to fractionating a polydisperse macromolecular solution. The underlying mechanism may also be operating at solid–liquid interfaces with small inorganic, organic, or biological particles exhibiting atomically flat surfaces.

Received: November 23, 1999

[1] J.-M. Lehn, *Science* **1993**, *260*, 1762.
[2] D. Ohilip, J. F. Stoddart, *Angew. Chem Int. Ed. Engl.* **1996**, *35*, 1154.
[3] A. Terfort, N. Bowden, G. M. Whitesides, *Nature* **1997**, *386*, 162.
[4] J. N. Israelachvili, *Intermolecular and Surface Forces*, 2nd ed., Academic, London **1992**.
[5] J. Sambrook, E. M. Fritsch, T. Maniatis, *Molecular Cloning: A Laboratory Manual*, 2nd ed., Cold Spring Harbor Laboratory, New York **1989**.
[6] P. J. Flory, *Principles of Polymer Chemistry*, Cornell University Press, New York **1953**.
[7] E. L Thomas, "Structure and Properties of Polymers", in *Materials Science and Technology—A Comprehensive Treatment* (Eds: R. W. Cahn, P. Haasen, E. J. Kramer), Wiley-VCH, Weinheim **1993**, Vol. 12.
[8] P. M. Cotts, T. M. Swager, Q. Zhou, *Macromolecules* **1996**, *29*, 7323.
[9] L. A. Bumm, J. J. Anrold, M. T. Cygan, T. D. Dunbar, T. P. Burgin, L. Jones, D. L. Allara, J. M. Tour, P. S. Weiss, *Science* **1996**, *271*, 1705.
[10] R. H. Friend, R. W. Gymer, A. B. Holmes, J. H. Burroughes, R. N. Marks, C. Taliani, D. D. C. Bradley, D. A. Dos Santos, J. L. Brédas, M. Lögdlund, W. R. Salaneck, *Nature* **1999**, *397*, 121.
[11] P. Samorí, V. Francke, K. Müllen, J. P. Rabe, *Chem. Eur. J.* **1999**, *5*, 2312.
[12] J. P. Rabe, S. Buchholz, *Science* **1991**, *253*, 424.
[13] K. Binder, *Montecarlo and Molecular Dynamics Simulations in Polymer Science*, Oxford University Press, Oxford **1995**.
[14] V. Palermo, F. Biscarini, C. Zannoni, *Phys. Rev. E* **1998**, *57*, R2519.
[15] G. J. Fleer, M. A. Cohen Stuart, J. M. H. M. Schentjens, T. Cosgrove, B. Vincent, *Polymers at Interfaces*, Chapman and Hall, London **1993**, p. 272.
[16] T. K. Xia, U. Landman, *Science* **1993**, *261*, 1310.
[17] A. Y. Grosberg, A. R. Khokhlov, *Giant Molecules Here, There Everywhere*, Academic, London **1997**, p. 73.
[18] W. Wang, G. Lieser, G. Wegner, *Liq. Cryst.* **1993**, *15*, 1.
[19] K. E. Huggins, S. Son, S. I. Stupp, *Macromolecules* **1997**, *30*, 5305.
[20] F. Rodriguez, *Principles of Polymer Systems*, Taylor and Francis, London **1996**, p. 200.
[21] A. Kothera, in *Polymer Fractionation* (Ed. M. J. Cantow), Academic, New York **1967**.
[22] C. E. Halkyard, M. E. Rampey, L. Kloppenburg, S. L. Studer-Martinez, U. H. F. Bunz, *Macromolecules* **1998**, *31*, 8655.
[23] Molecular modelling package *Discover*, Version 4.0.0, Biosym. Technologies Inc., San Diego, CA.

Uniform Nickel Deposition into Ordered Alumina Pores by Pulsed Electrodeposition**

By *Kornelius Nielsch*, *Frank Müller*, *An-Ping Li*, and *Ulrich Gösele**

The fabrication of nanoscale structures has attracted much interest recently owing to their potential use in high-density magnetic memories,[1,2] single-electron devices,[3] nanoelectrodes for the direct deposition of nanoparticles from the gas phase,[4] and optical media.[5] A periodic pore arrangement in porous anodic alumina was first reported by Masuda et al. in 1995.[6] The production of nanostructures based on hexagonally arranged porous alumina as a mask or matrix structure is cheaper than that based on traditional methods like nanoscaling using electron beam lithography.[7] To use such an alumina template for new applications of nanostructures, the pores have to be filled with a conducting or semiconducting material, for example via electrochemical deposition. In contrast to other deposition methods like chemical vapor deposition (CVD), during electrochemical deposition the growth of nanowires starts at the pore tips and continues in the pore direction from the pore bottom to the pore opening.

The electrochemical deposition of a metallic or semiconducting material on an insulating and rather thick barrier layer (1–1.2 nm per volt oxidation potential[8]) at the pore tips is not straightforward. The periodically arranged alumina structures (oxidation potential 20–195 V)[9–14] exhibit a thick barrier layer unlike the unarranged structures (10–20 V) used, for example, for solar absorbers.[5] High potentials are required for the tunneling of the electrons through the barrier layer. Electrodeposition by direct current (DC) is very unstable and uniform filling of the pores cannot be achieved. This is due to a cathodic side reaction, which leads to a partial removal of the barrier oxide, formation of holes in the barrier layer, and local deposition in single pores.

Until now, two different methods have been developed to obtain uniform and complete filling of pores by electrodeposition. In the first method, a direct current is used for the deposition.[15,16] Therefore, the porous alumina needs to be detached from the aluminum substrate. Subsequently, the barrier layer is removed from the matrix structure by a chemical etching process. As a final pre-treatment step for the filling process, a metallic contact is sputtered on one side of the free-standing alumina membrane. The concept of transferring the alumina membrane is only applicable for free-standing membranes that are thick (>20 μm) and stable enough to be handled. For most of the nanostructure applications mentioned above, a porous alumina thickness of only a few hundred nanometers is required.

In this work, the second method used for filling the alumina pores was first developed by Caboni.[17–19] This method has been used for the coloration of anodic alumina in industry. Porous alumina remains on the aluminum substrate and the metal is deposited on the barrier layer at the pore tips by an alternating deposition potential.[1,2,7,19,20] In this case, the production of ordered and metal-filled alumina pore structures is not limited by the thickness and size of the barrier oxide and its rectifying contact allows metal deposition by an alternating potential. Furthermore, in aqueous deposition solutions, the high cathodic potentials cause some hydrogen evolution, which may inhibit the deposition.[19,20] Therefore, we have adopted the concept of pulsed electrodeposition (PED),[21–24] which is reliable for deposition into high aspect materials and which can compensate for the slow diffusion-driven transport in the pores.

[*] Prof. U. Gösele, K. Nielsch, Dr. F. Müller, Dr. A.-P. Li
Max-Planck-Institut für Mikrostrukturphysik
Weinberg 2, D-06120 Halle (Germany)

[**] The authors thank Mrs. S. Hopfe for the SEM sample preparations and Dr. S. Senz and Mrs. S. Reichel for the X-ray measurements.

 © WILEY-VCH Verlag GmbH, D-69469 Weinheim, 2000 0935-9648/00/0804-0582 $ 17.50+.50/0

ADVANCED MATERIALS

The method is commonly used for the electrodeposition of thin metallic films. For the first time, this technique is applied in combination with a highly ordered nanostructured template material.

The hexagonally ordered porous alumina membranes have been prepared via a two-step anodization process, which is described in detail elsewhere.[13,14] A first long-duration anodization causes the formation of channel-arrays with a high aspect ratio and a regular pore arrangements via self-organization.[9–14] After complete dissolution of the oxide structure (Fig. 1a), the surface of the aluminum substrate keeps the regular hexagonal texture of the self-organized pore tips, which act as a self-assembled mask

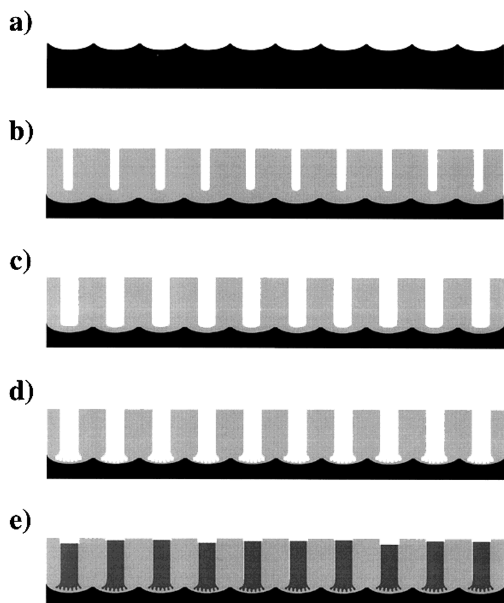

Fig. 1. Schematic diagram describing the fabrication of a highly ordered porous alumina matrix and the preparative steps necessary for the subsequent filling of the structure. a) The Al substrate was pre-structured by anodizing for a long period of time and removing the oxide. b) A highly ordered alumina pore structure was obtained in a second anodization step. c) The barrier layer was thinned and the pores were widened by isotropic chemical etching. d) For further thinning of the barrier layer two current-limited anodization steps were used and dendrite pore formation occurred at the barrier layer. e) Pulsed electrodeposition of nickel in the pores.

for a second anodization process. After a second anodization for 1 h, an ordered nanopore array (Fig. 1b) is obtained with straight pores from top to bottom and a thickness of typically 1 µm. The parameters are 0.3 M oxalic acid, U_{ox} = 40 V, and T = 2 °C. The measured anode current is plotted in Figure 2. It is almost stable after the formation of the barrier oxide (minimum of the current–time curve). During the course of anodization, the oxide dissolution and formation rate are in equilibrium at the barrier layer, thus the anode current and thickness of the barrier layer remains stable. The measured current is approximately proportional to the anodization voltage under these equilibrium conditions. The interpore distance (2.6 nm/V) and the thickness of the barrier layer (1.3 nm/V) are proportional to the applied cell potential.

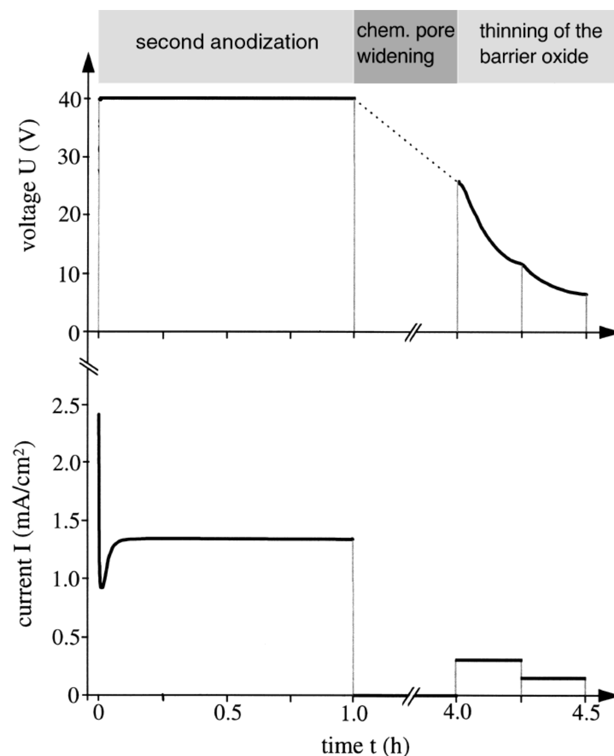

Fig. 2. Voltage–time and current–time curves for the second anodization (T = 2 °C), chemical pore widening (T = 30 °C), and the thinning of the barrier layer (T = 2 °C) in 0.3 M oxalic acid.

By thinning the barrier layer the quality and the homogeneity of the deposition process in the pores is significantly improved. We assume that thickness fluctuations of the barrier layer are smoothened by this treatment step. The thinning leads to a considerable decrease in the potential barrier for the electrons to tunnel through the barrier layer, when the metal is deposited at the pore tips. Thus, lower voltages are necessary for the electrochemical filling of the pores and the pore matrix can be maintained on the aluminum substrate.

The barrier layer is thinned by chemical pore widening and by current limited anodization steps. First, the oxalic acid is heated up to 30 °C to decrease the thickness of the barrier layer by chemically widening the pores (Fig. 1c). After 3 h, the barrier layer decreases to 30 nm and the mean pore diameter increases to approximately 50 nm, which could be calculated from the anodizing potential of about 25 V (Fig. 2). Then, the electrolyte is cooled down to 2 °C to interrupt the widening process. Depending on the required pore diameter the chemical pore widening can be omitted.

Second, the structure is anodized twice for 15 min using constant current conditions at 290 and 135 mA/cm^2. The anodization is carried out under non-equilibrium conditions. The thickness of the barrier layer (Fig. 1d) and the anodizing potential (Fig. 2) both decrease. The formation rate of the oxide is limited by the applied current. The ratio of the dissolution rate to the formation rate of the oxide is higher under these conditions than for anodization under a

 © WILEY-VCH Verlag GmbH, D-69469 Weinheim, 2000 0935-9648/00/0804-0583 $ 17.50+.50/0

constant cell potential, until a new equilibrium of these two processes is reached and the thickness of the barrier layer becomes stable. Finally, the anodizing potential reaches a value of 6–7 V, which corresponds with a barrier oxide thickness of less than 10 nm. Further reduction of the anodizing potential may cause the oxide structure to completely peel off of the metal substrate during the deposition.

During the current-limited anodization, the pores branch out at the formation front because the equilibrium number of pores per square centimeter is inversely proportional to the square of the anodizing potential.[8,12] We suppose that the split-up of the pores in the layer between the ordered alumina structure and the aluminum substrate favors the formation of several nucleation sites in each pore at the beginning of the electrodeposition.

The metal is electrodeposited from an aqueous electrolyte at the pore tip of our high aspect-ratio porous material (Fig. 1e). The rectifying properties of the barrier layer allow the pores to be filled uniformly by AC or pulsed electrodeposition. Experimental investigations have shown that using direct current for the deposition fills the pores non-uniformly.[20] For DC deposition, the applied potentials are smaller than for pulsed (PED) or AC deposition. The potential of the electrons, which drops across the barrier layer during the deposition, depends on the thickness of the barrier layer. Therefore a higher proportion of the applied deposition potential drops across the barrier layer in the case of DC deposition and thus thickness fluctuations of the barrier layer influence the deposition rate in each pore more strongly.

The formation of hydrogen can become more dominant for PED or AC deposition.[20,25] This effect, however, can be minimized if the deposition interfaces are being supplied sufficiently with metal ions during the course of deposition. Instead of the frequently used AC deposition,[1,2,5,7,19,20,25] the PED concept was used for the filling of porous alumina. In contrast to alternating voltage pulses, in PED current pulses were applied, which allowed better control over the deposition parameters, such as deposition rate and ion concentration at the deposition interface.

While metal is deposited at the pore tips, the metal ions are exhausted with decreasing ion concentration. Along each pore the concentration grows, but for the metal ions it takes time to migrate from the pore opening to the pore ground via thermal diffusion. The number of metal ions exhausted during one deposition pulse was estimated by a simple procedure. The following parameters were used for the calculation: concentration of metal ion c_{me} = 1.33 M, membrane thickness h = 1 μm, porosity p = 30 %, deposition current I_{pulse} = 70 mA/cm^2, pulse time t_{pulse} = 8 ms, and 100 % current efficiency. As a result, in the area at the pore tip and within 70 nm practically all the metal ions should be deposited during one pulse. This is about 7 % of all the metal ions in our membrane structure. Consequently, a relatively long delay time, t_{off}, has been inserted between two successive deposition pulses, sufficient for the concentration of metal ions at the pore tips to recover and for the deposition interfaces to be supplied with ions again, before the next deposition pulse starts. If the rate of electrodeposition is higher than that of the transport through the pores, the metal ion concentration decreases at the bottom of the pores. Consequently, hydrogen evolution becomes the dominant process, inhibiting the homogeneous deposition and decreasing the pore filling factor and the current efficiency.

Using a highly concentrated electrolyte increases further the concentration of metal ions at the pore tips. Consequently, we use the so-called Watts bath,[26] which is a mixture of 300 g/L $NiSO_4 \cdot 6H_2O$, 45 g/L $NiCl_2 \cdot 6H_2O$, 45 g/L H_3BO_3, pH 4.5. The electrolyte temperature is 35 °C. The mixture is very similar to the less concentrated electrolytes that were used earlier for the metal electrodeposition into porous alumina at room temperature.[1,2] The Watts bath contains boric acid, which is known as an electrolyte to form very stable oxide layers. As a beneficial effect, discontinuities of the barrier layer could be repaired during positive polarization.[19]

The deposition was based on modulated pulse signals in the microsecond range (Fig. 3). During the relatively long pulse of negative current (8 ms, I_{pulse} = –70 mA/cm^2) the metal is deposited on the pore ground. In comparison to the direct current deposition, relatively high current densities are applied at the moment of metal deposition, which should increase the number of deposition centers in each pore.[21] Figure 3 shows the applied negative current pulse (a) and the measured signal of the potential (b). After a short abrupt rise in the negative deposition voltage this measured absolute value of the signal increases a little further, which is due to the charging of the capacitance of the barrier layer and the depletion of metal ions near the deposition interface. The voltage signal varied between –8 and –12 V.

After the deposition pulse, a short pulse of positive polarization (2 ms, U_{pulse} = +3 V) (Fig. 3b) follows to discharge the capacitance of the barrier layer and to immediately interrupt the electric field at the deposition interface. The current is limited to I_{max} = ±70 mA/cm^2 for both pulses. Consequently, this measured current signal (Fig. 3a) deviates slightly from the ideal form of an exponential discharging curve of a capacitor. As mentioned above, the positive pulse also repairs discontinuities in the barrier layer.

The delay time, t_{off}, was varied between 10 ms and 5 s. During this period the ion concentration recovers. Thus, the concentration of metal ions is high at the bottom of each pore when the subsequent deposition pulse appears. The delay time, t_{off}, improves the homogeneity of the deposition and limits the hydrogen evolution. The deposition was continued up to the drop in the deposition potential, which was due to the beginning of nickel deposition on top of the matrix structure.

© WILEY-VCH Verlag GmbH, D-69469 Weinheim, 2000
0935-9648/00/0804-0584 $ 17.50+.50/0

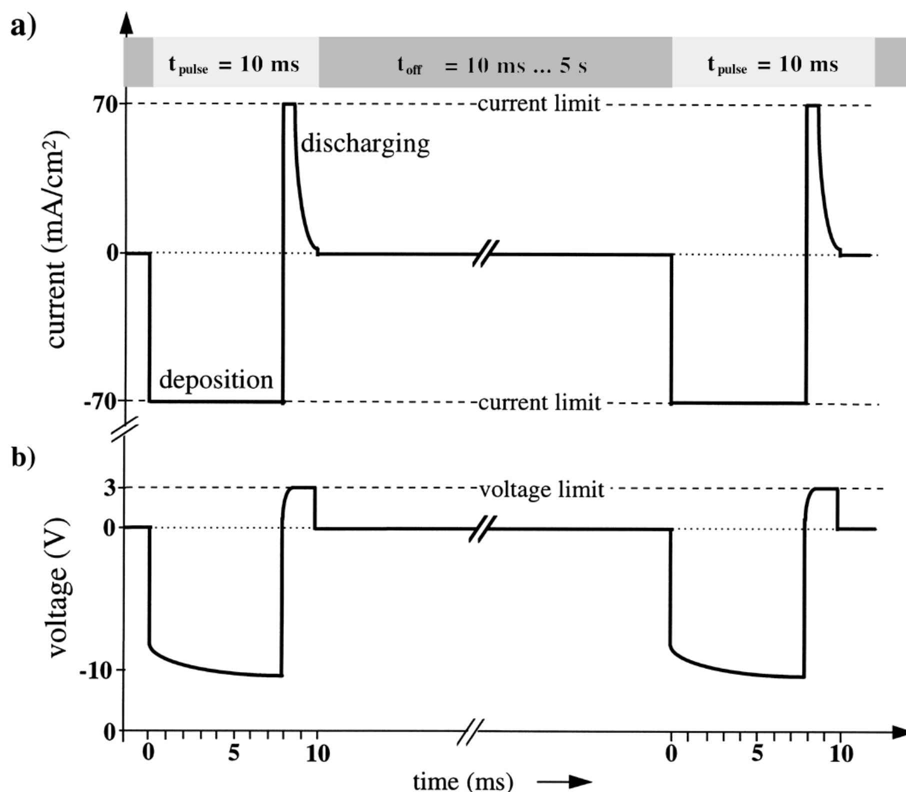

Fig. 3. Schematic diagram of the filling of porous alumina structure with nickel by pulsed electrodeposition. The deposition of nickel starts at the thinned barrier layer.

The filled alumina samples were examined by scanning electron microscopy (SEM) to determine the degree of pore filling and the extension of the nickel nanowires. By thinning the filled porous alumina from the top, nanowires ending below the matrix surface became observable for SEM investigation. Thinning the sample by a focused ion beam yielded a 100 nm deep and funnel-shaped excavation in the structure. The depth of the hole is calculated from the thinning time. As micrographs of the filled pores are taken at different depths beneath the initial membrane surface, an overview was obtained about the extent of nanowires along the pore axis and the length distribution of the nanowires was evaluated. Before the SEM investigations, a thin gold film of a few nanometers thickness was sputtered onto the filled structure to enhance the surface conductivity for the SEM observations.

Figure 4 shows top view SEM micrographs of a highly ordered alumina pore structure filled with nickel. For electrodeposition in the pores of this sample, a delay time t_{off} = 990 ms was chosen. The measured pore diameter is between 45 and 55 nm and the pore distance is 110 nm. Figure 4a shows a region outside the thinned area and in some pores the nickel nanowires have grown up to the pore opening. Figure 4b shows a micrograph of an area about 50 nm below the initial surface. Finally, the lowest point of the excavation is shown (Fig. 4c), where a layer of 100 nm has been removed from the 1 μm thick membrane.

Almost 100 % of the pores are filled with nickel (Fig. 4c). Away from this lowest level, where the structure was less thinned, metal filling can be detected in fewer pores (Fig. 4a). Nevertheless, if this micrograph (Fig. 4a) is compared with Figure 4c, it can be seen that almost every pore of the alumina structure was filled with nickel. In the black colored pores in Figure 4a and Figure 4b the nickel nanowires end beneath the pore opening. If we take into account that the thickness of the structure was only decreased by about 10 % at the lowest etched level (Fig. 4c), the lengths of the nickel nanowires are more than 90 % (900 nm) of the membrane thickness and fluctuate slightly. This assumption is also supported by Fig. 4a, where the gray level of the filled pores fluctuates slightly. The different gray levels are caused by nickel fillings, which end at (white color) or a few nanometers below (gray color) the matrix surface.

When the deposition is carried out using a short t_{off} = 10–100 ms, in a few pores the wire growth is particularly pronounced. To reach a level at which nickel filling can be observed in most of the pores, the sample thickness had to be decreased to less than 30 % of the initial value. Close to the barrier layer, approximately 100 % of the pores are filled. At the beginning of the deposition process, the splitting of the pores at the bottom of the alumina membrane allows the formation of several nucleation centers in each pore. Nevertheless, for short t_{off} the growth rate of the metal filling fluctuates considerably. Under these deposition parameters, we also observed the formation of hydrogen bubbles on the membrane surfaces during the depositions. This may be due to the depletion of the metal ion concentration at the deposition interface, which leads to an increased evolution of hydrogen in the pores and disturbs the diffusion of ions in the pores. Therefore, the nickel is preferentially deposited in a few pores and the lengths of the wires varies considerably.

A sufficiently long relaxation time t_{off} between the pulse sequences ensures uniform material transport through the pores, refreshes the concentration of metal ions at the deposition interface and leads to uniform wire growth. On the other hand, when t_{off} is prolonged, the total deposition time also increases and the pores stay in contact with the electrolyte for a longer time. For t_{off} > 2 s, a peeling-off of macroscopic pieces of porous alumina is observed. A chem-

 © WILEY-VCH Verlag GmbH, D-69469 Weinheim, 2000 0935-9648/00/0804-0585 $ 17.50+.50/0

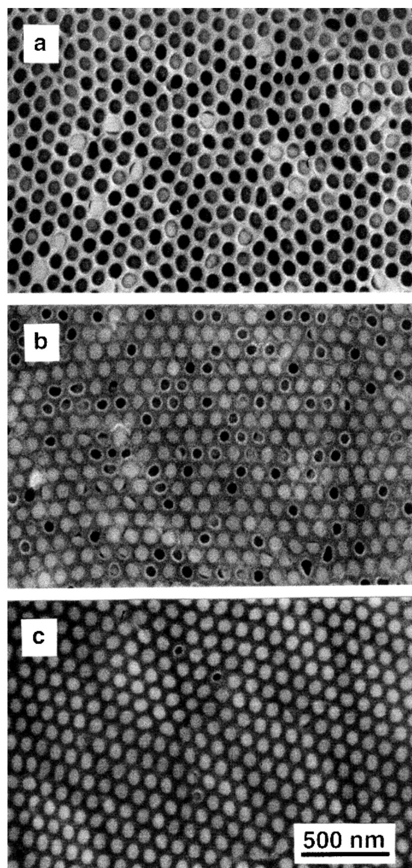

Fig. 4. Top view SEM micrographs of a nickel-filled alumina membrane, t_{pulse} = 10 ms, t_{off} = 0.99 s, membrane thickness = 1 µm: a) unthinned, b) 50 nm, and c) 100 nm underneath the initial surface.

ical side reaction between the oxide and the electrolyte seems to be dominant for these long duration depositions.

As a result, we obtained the best nickel filling in the membranes for t_{off} of about 1 s. The crystallinity of this sample was further analyzed by X-ray diffraction (XRD). From the θ–2θ scan we have made a simple estimate of the average crystallite size by the Scherrer equation for round particles. For the Ni (111) peak a particle diameter D_p = 13.7 nm and for the (200) peak D_p = 12.5 nm was calculated. These values are in good agreement with data reported earlier for the PED of thin nickel films.[22,24]

The method of pulsed electrodeposition can also be applied to other materials like Fe, Co, and NiFe-alloys, which are interesting ferromagnetic materials for high-density magnetic memory. Moreover, it is possible to dissolve the porous alumina host using a mixture of phosphoric and chromic acid to set free these monodisperse metal nanowires.

In summary, a highly efficient method for deposition of nickel into ordered nanochannels of porous alumina has been presented. By thinning the barrier layer homogeneously, the porous structure could be kept on the aluminum substrate for the whole process. Our approach to the fabrication of a highly ordered metal nanowire array is inexpensive and very flexible with respect to the size and thickness of the pore structure. In addition, the thickness of the barrier layer and the pore diameter could in principle be varied independently of each other. The use of pulsed electrodeposition is well-suited for a uniform deposition in the pores of porous alumina structures, as demonstrated for nickel electrodeposition. Nearly 100 % of the pores were filled with nanocrystalline nickel and only a very small fluctuation in growth rate of these nanowires was observed. XRD measurement confirmed the crystallinity of the filling. It is expected that this fabrication process can also be applied to the deposition of other metals and semiconductors for the synthesis of nanowire systems. In particular Co, Fe, and NiFe are promising filling materials, which could lead to high-density magnetic memories.

Received: November 3, 1999
Final version: January 24, 2000

[1] D. Al Mawlawi, N. Coombs, M. Moskovits, *J. Appl. Phys.* **1991**, *70*, 4421.
[2] F. Li, R. M. Metzger, W. D. Doyle, *IEEE Trans. Magn.* **1997**, *33*, 3715.
[3] A. A. Tager, J. M. Xu, M. Moskovits, *Phys. Rev. B* **1997**, *55*, 4530.
[4] F. E. Kruis, K. Nielsch, H. Fissan, B. Rellinghaus, E. F. Wasserman, *Appl. Phys. Lett.* **1998**, *73*, 547.
[5] E. Wäckelgård, *J. Phys.: Cond. Matter* **1996**, *8*, 5125.
[6] H. Masuda, K. Fukuda, *Science* **1995**, *268*, 1466.
[7] D. Routkevitch, A. A. Tager, J. Haruyama, D. Almawlawi, M. Moskovits, J. M. Xu, *IEEE Trans. Electron Devices* **1996**, *147*, 1646.
[8] F. Keller, M. S. Hunter, D. L. Robinson, *J. Electrochem. Soc.* **1953**, *100*, 411.
[9] O. Jessensky, F. Müller, U. Gösele, *Appl. Phys. Lett.* **1998**, *72*, 1173.
[10] O. Jessensky, F. Müller, U. Gösele, *J. Electrochem. Soc.* **1998**, *145*, 3735.
[11] H. Masuda, F. Hasegawa, S. Ono, *J. Electrochem. Soc.* **1997**, *144*, L127.
[12] A. P. Li, F. Müller, A. Birner, K. Nielsch, U. Gösele, *J. Appl. Phys.* **1998**, *84*, 6023.
[13] H. Masuda, K. Yada, A. Osaka, *Jpn. J. Appl. Phys.* **1998**, *37*, L 1340.
[14] A. P. Li, F. Müller, A. Birner, K. Nielsch, U. Gösele, *Adv. Mater.* **1999**, *11*, 483.
[15] H. Masuda, M. Yotsuya, M. Ishida, *Jpn. J. Appl. Phys.* **1998**, *37*, L1090.
[16] O. Jessensky, *PhD Thesis*, Martin-Luther-University of Halle, Germany **1997**.
[17] V. Caboni, *Italian Patent 339 232*, **1936**.
[18] Langbein-Pfandhauser GmbH, *German Patent 741 753*, **1940**.
[19] W. Sautter, G. Ibe, J. Meier, *Aluminium* **1974**, *50*, 143.
[20] D. Routkevitch, J. Chan, J. M. Xu, M. Moskovits, *Electrochem. Soc. Proc. Ser.* **1997**, *PV 97-7*, 350.
[21] J. C. Puippe, F. Leaman, *Theory and Practice of Pulse Plating*, AESF, Orlando **1986**.
[22] G. McMahon, U. Erb, *Microstruct. Sci.* **1989**, 17, 447.
[23] H. Natter, M. Schmelzer, R. Hempelmann, *J. Mater. Res.* **1998**, *13*, 1186.
[24] P. T. Tang, T. Watanabe, J. E. T. Andersen, G. Bech-Nielsen, *J. Appl. Electrochem.* **1995**, *25*, 347.
[25] D. Ebling, J. W. Schulze, *Metalloberflächen* **1990**, *44*, 491.
[26] O. P. Watts, *Trans. Am. Electrochem. Soc.* **1916**, *29*, 395.

 © WILEY-VCH Verlag GmbH, D-69469 Weinheim, 2000 0935-9648/00/0804-0586 $ 17.50+.50/0